

Rotational line strengths for the cyanide $B^2\Sigma - X^2\Sigma^+ (5,4)$ band

 James O Hornkohl¹ and Christian G Parigger^{2*}
¹Hornkohl Consulting, 344 Turkey Creek Road, Tullahoma, TN, USA

²University of Tennessee, University of Tennessee Space Institute, Center for Laser Applications, Tullahoma, TN, USA

Received: March 03, 2017; Accepted: April 06, 2017; Published: April 13, 2017

***Corresponding author:** Christian Parigger, Associate Professor, University of Tennessee, University of Tennessee Space Institute, Center for Laser Applications, 411 B.H. Goethert Parkway, Tullahom, TN 37388-9700, USA, Tel: (931)393-7338/509; E-mail: cparigge@tennessee.edu

Abstract

Rotational line strengths, computed from eigenvectors of Hund's case (a) matrix representations of the upper and lower Hamiltonians using Wigner-Witmer basis functions, show a larger than expected influence from the well-known perturbation in the (5,4) band. Comparisons with National Solar Observatory experimental Fourier transform spectroscopy data reveal nice agreement of measured and predicted spectra.

Keywords: Diatomic Spectroscopy; Rotational line strengths; Hönl-London factors; Cyanide spectra violet band perturbations;

Introduction

The CN violet $B^2\Sigma^+ - X^2\Sigma^+$ band system is one of the most studied band systems. Ram, et al. [1] and Brooke, et al. [2] reported experimental results and theoretical information, respectively. Of the many known bands in the violet system, only the (5,4) band is considered here. This band exhibits a weak, quantitatively understood perturbation [4] caused by mixing of the $v=17$ level of $A^2\Pi$ with the $v=5$ level of $B^2\Sigma^+$. The particular perturbation of the CN (5,4) band is evaluated in this work by isolating the spectral features of this band that is part of the CN violet system.

Methods

Numerical diagonalizations of upper and lower Hamiltonians with and without the perturbation are investigated and compared with available experimental spectra. The simulations rely on determining rotational strengths without parity-partitioned Hamiltonians. It is anticipated that the investigated (5,4) band modifications can be possibly confirmed with the new PGOPHER program recently released by Western [3].

For the computation of rotational spectra, the square of transition moments are numerically computed using the eigenvectors of upper and lower Hamiltonians. This approach

can also be selected in the new PGOPHER program [3]. For the diatomic molecule, the results effectively yield the Hönl-London factors yet we do not utilize tabulated Hönl-London factors that are available in standard textbooks.

Results

CN (5,4) band spectra

Table 1: Lines in the CN $B^2\Sigma^+ - X^2\Sigma^+$ (5,4) band near the perturbation. $\tilde{\nu}$ are the fitted line positions, $S(J', J)$ are the rotational line strengths computed in the fitting algorithm. Without spin-orbit mixing, $S^{(0)}(J', J)$ and $\Delta\tilde{\nu}^{(0)}$ are the line strengths and differences of the fitted line positions, respectively. Spin-orbit mixing of $B^2\Sigma^+$ and $A^2\Pi$ shifts the upper \mathcal{E} parity levels, and significantly reduces the differences, $\Delta\tilde{\nu}$, between measured and computed line positions.

J'	J		p'	$\tilde{\nu}$	S_{JJ}	$\Delta\tilde{\nu}$	$S_{JJ}^{(0)}$	$\Delta\tilde{\nu}^{(0)}$
9 ½	8 ½	R_1	-e	28013.117	9.474	-0.010	9.474	0.337
9 ½	8 ½	R_2	+f	28017.421	9.474	0.001	9.474	-0.059
10 ½	9 ½	R_1	+e	28016.992	9.199	-0.004	10.476	0.600
10 ½	9 ½	R_2	-f	28021.651	11.171	-0.000	10.476	-0.067
11 ½	10 ½	R_1	-e	28020.540	7.868	-0.041	11.478	1.193
11 ½	10 ½	R_2	+f	28025.866	12.240	0.006	11.478	-0.067
12 ½	11 ½	R_2	-f	28030.125	13.288	0.007	12.480	-0.072
12 ½	11 ½	R_1	+e	28030.431	13.812	0.000	12.480	0.000
13 ½	12 ½	R_1	-e	28032.081	17.455	-0.053	13.481	-1.870
13 ½	12 ½	R_2	+f	28034.428	14.325	0.011	13.481	-0.073
14 ½	13 ½	R_1	+e	28035.672	17.919	-0.005	14.483	-1.102
14 ½	13 ½	R_2	-f	28038.773	15.356	0.013	14.483	-0.076
15 ½	14 ½	R_1	-e	28039.742	18.442	0.007	15.484	-0.807
15 ½	14 ½	R_2	+f	28043.161	16.383	0.009	15.484	-0.084
16 ½	15 ½	R_1	+e	28043.989	19.132	0.011	16.485	-0.655
16 ½	15 ½	R_2	-f	28047.590	17.405	0.006	16.485	-0.091

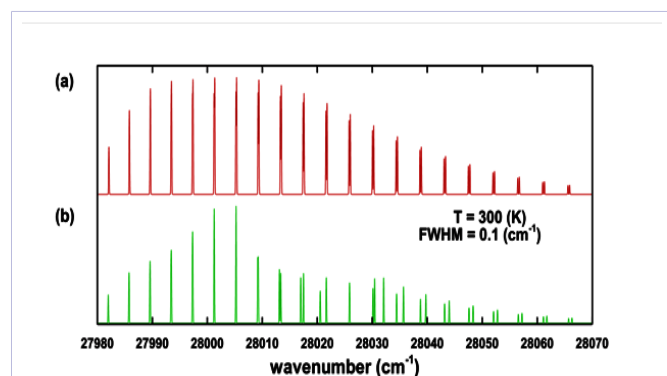


Figure 1: Synthetic emission spectra. (a) pure upper states $^2\Sigma^+$; (b) upper states are treated as the sum $c_2\ ^2\Sigma^+ + c_1\ ^2\Pi$ with $c_2 > c_1$. Only R branch lines are shown, including those given in Table 1.

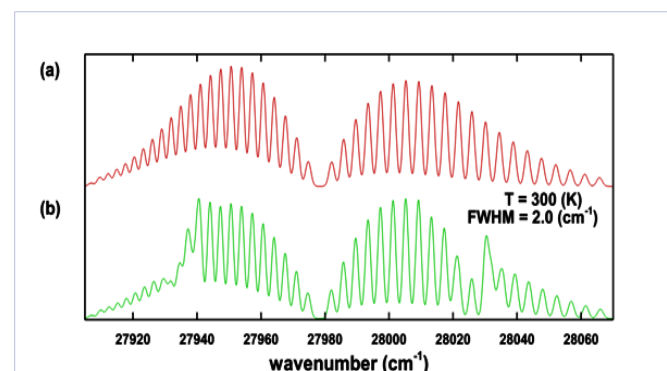


Figure 2: Computed spectra for P and R branches. (a) pure and (b) perturbed upper states.

Table 1 and Figures 1 and 2 show the results obtained with and without taking into account the mixing. In Table 1, lines of the CN $(5,4)$ band are listed that are spectrally close to the perturbation. Comparisons of line positions, $\tilde{\nu}$, and the rotational line strengths, $S(J',J)$, with the corresponding unperturbed values, $S^{(0)}(J',J)$, are presented. The differences, $\Delta\tilde{\nu}^{(0)}$, for which the off-diagonal spin-orbit coupling constants $\langle AL \rangle$ and $\langle BL \rangle$ are set equal to 0, are significantly larger than the usual differences, $\Delta\tilde{\nu}$, of computed and experimentally determined line positions. The spin-orbit mixing of $B^2\Sigma^+$ and $A^2\Pi$ shifts the upper parity levels. Table 3 also shows that a relatively large fractional error, e.g., $-3.974/17.455$ versus $-1.870/28032$ for $R_{11}(J=12.5)$ can occur in the computed rotational line strengths, $S(J',J)$. Figure 1 displays the computed spectra of only the R branch in the range of 27980 to 28070 cm^{-1} , including the lines listed in Table 1 with and without spin-orbit mixing. The $\nu=17, A^2\Pi$ energy eigenvalues lie very near the $\nu=5, B^2\Sigma^+$ eigenvalues, and this causes a significant effect from the $A^2\Pi$ level. Figure 2 illustrates computed spectra for P and R branches in the range of 27905 to 28070 cm^{-1} for pure and perturbed upper states. The perturbed states are affected by the addition of a small amount of $^2\Pi$ states to the upper level basis. Clearly, the perturbations reveal noticeable differences in the appearance of the violet $(5,4)$ band even at low, 2.0 cm^{-1} , resolution.

Results of modeling the angular momentum states of the upper $\nu=5$ vibrational level as a mixture of $^2\Sigma$ and $^2\Pi$ Hund's case (a) basis functions, a so-called "de-perturbation" or perturbation analysis, agree well that of Ito, et al. [4] who used the line position measurements of Engleman [5]. The 100 lines of the more recent data of Ram, et al. [1] were fitted with a standard deviation of cm^{-1} . The standard deviation would be increased from 0.025 to 0.25 cm^{-1} without the inclusion of spin-orbit mixing of the $B^2\Sigma^+$ and $A^2\Pi$ basis states.

Changes in the spectra are relatively larger for the rotational line strengths, $S(J',J)$ for the line positions, $\tilde{\nu}$. The simulation results compare nicely with measured spectra [1] available from the National Solar Observatory (NSO) at Kitt Peak [6]. Figure 3 displays the recorded and simulated spectra for a resolution of 0.03 cm^{-1} . The Fourier transform spectrum 920212R0.005 [6] was recorded [1] at a temperature of 20.5 degree Celsius, or at 293.65 Kelvin, and at a spectral resolution of 0.03 cm^{-1} . The corresponding R branch spectrum is computed for a temperature of 300 K and it compares nicely with the recorded data. The predicted line positions of the R branch match the vacuum wavenumbers of the experimental spectrum.

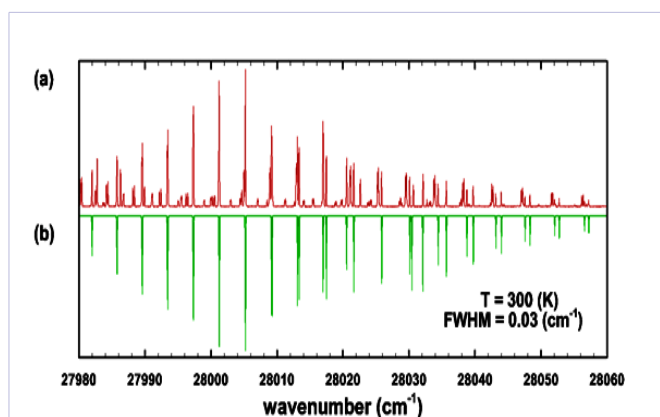


Figure 3: Measured and simulated spectra. (a) Segment of the recorded [1] Fourier transform spectrum 920212R0.005 [6], (b) computed spectrum for a temperature of 300 K and a spectral resolution of 0.03 cm^{-1} . The computed $(5,4)$ R branch is flipped vertically for ease of comparisons.

The influence of $^2\Sigma + ^2\Pi$ mixing on the rotational line strengths, $S(J',J)$, can be recognized because computation of $S(J',J)$ is an integral part of the unique line position fitting algorithm. Upper and lower Hamiltonian matrices in the Hund's case (a) basis are numerically diagonalized, and the spectral line vacuum wavenumber $\tilde{\nu}$ is the difference between upper and lower Hamiltonian eigenvalues. To determine which of the many eigenvalue differences represent allowed spectral lines, the factor $S(J',J)$ is computed from the upper and lower eigenvectors for each eigenvalue difference. A non-vanishing $S(J',J)$ denotes an allowed diatomic spectral line. Parity partitioned effective Hamiltonians are not used. Parity and branch designation are not required in the fitting algorithm. Input data to the fitting program is a table of vacuum wavenumber $\tilde{\nu}$ versus J' and J .

The non-vanishing of the rotational strength is the only selection rule used. Applications of this rule leads to the establishment of spectral data bases for diatomic molecular spectroscopy of selected transitions [7]. Over and above the PGOPHER program [3], there are other extensive efforts in predicting diatomic molecular spectra including for instance the so-called Duo program [8] for diatomic spectroscopy.

Wigner-Witmer diatomic eigenfunction

The Hund's case (a) basis functions were derived from the Wigner and Witmer [9] diatomic eigenfunction,

$$\langle \rho, \zeta, \chi, \mathbf{r}_2, \dots, \mathbf{r}_N, r, \theta, \varphi | n\nu JM \rangle = \sum_{\Omega=-J}^J \langle \rho, \zeta, \mathbf{r}'_2, \dots, \mathbf{r}'_N, r | n\nu \rangle D_{M\Omega}^{\nu*}(\varphi, \theta, \chi). \quad (1)$$

The coordinates are: The distance ρ of one electron (the electron arbitrarily labeled 1 but it could be any one of the electrons) from the internuclear vector $\mathbf{r}(r, \theta, \varphi)$ the distance ζ of that electron above or below the plane perpendicular to \mathbf{r} , and passing through the center of mass of the two nuclei (the coordinate origin), the angle χ for rotation of that electron about the internuclear vector \mathbf{r} , and the remaining electronic coordinates $\mathbf{r}_2, \dots, \mathbf{r}_N$ in the fixed and $\mathbf{r}_2, \dots, \mathbf{r}_N$ in the rotating coordinate system.

The vibrational quantum number ν has been extracted from the quantum numbers collection n that represents all required quantum numbers except J , M , Ω , and ν . The Wigner-Witmer diatomic eigenfunction has no application in polyatomic theory, but for the diatomic molecule the exact separation of the Euler angles is a clear advantage over the Born-Oppenheimer approximation for the diatomic molecule in which the angle of electronic rotation, θ and φ . Equation (1) can be derived by writing the general equation for coordinate (passive) rotations α , β , and γ of the eigenfunction, replacing two generic coordinate vectors with the diatomic vectors $\mathbf{r}(r, \theta, \varphi)$ and $\mathbf{r}(\rho, \zeta, \chi)$, and equating the angles of coordinate rotation to the angles of physical rotation φ , θ and φ . The general equation for coordinate rotation holds in isotropic space, and therefore the quantum numbers J , M , and Ω in the Wigner-Witmer eigenfunction include all electronic and nuclear spins. If nuclear spin were to be included, J , M and Ω would be replaced by F , M_F , and Ω_F but hyperfine structure is not resolved in the (5,4) band data reported by [1], and Eq. (1) is written with the appropriate spectroscopic quantum numbers.

It is worth noting that the rotation matrix element

$D_{M\Omega}^{\nu*}(\varphi, \theta, \chi)$ and its complex conjugate $D_{M\Omega}^{\nu}(\varphi, \theta, \chi)$ do not fully possess the mathematical properties of quantum mechanical angular momentum. It is well known that a sum of Wigner D -functions is required to build an angular momentum state. The equation.

$$J_{\pm}' D_{M\Omega}^{\nu*}(\varphi, \theta, \chi) = \sqrt{J(J+1) - \Omega(\Omega \mp 1)} D_{M, \Omega \mp 1}^{\nu*}(\varphi, \theta, \chi) \quad (2)$$

is not a phase convention [10-12] but a mathematical result readily obtained from Eq. (1) and

$$J_{\pm}' | J\Omega \rangle = \sqrt{J(J+1) - \Omega(\Omega \pm 1)} | J, \Omega \pm 1 \rangle, \quad (3)$$

in which the prime on the operator J_{\pm}' indicates that it is written in the rotated coordinate system where the appropriate magnetic quantum number Ω

Hund's basis function

The Hund's case (a) basis function based upon the Wigner-Witmer diatomic eigenfunction is

$$| a \rangle = \langle \rho, \zeta, \chi, \mathbf{r}'_2, \dots, \mathbf{r}'_N, r, \theta, \varphi | n\nu JMS\Lambda\Sigma\Omega \rangle = \sqrt{\frac{2J+1}{8\pi^2}} \langle \rho, \zeta, \mathbf{r}'_2, \dots, \mathbf{r}'_N, r | n\nu \rangle | S\Sigma \rangle D_{M\Omega}^{\nu*}(\varphi, \theta, \chi). \quad (4)$$

As noted above, a sum of basis functions is required to build an eigenstate of angular momentum. The basis function would also not be an eigenstate of the parity operator. The case (a) matrix elements, $p_{ij}^{(a)}$, of the parity operator P ,

$$p_{ij}^{(a)} = p_{\Sigma} (-)^J \delta(J_i J_j) \delta(\Omega_i, -\Omega_j) \delta(\Lambda_i, -\Lambda_j) \delta(n_i n_j), \quad (5)$$

show that a single $| a \rangle$ basis function is not an eigenstate of parity. The procedure called parity symmetrization adds $| JM\Omega \rangle$ and $| JM, -\Omega \rangle$ basis functions thereby destroying the second magnetic quantum number Ω and yielding a function which at least possesses the minimal mathematical properties of an eigenstate of angular momentum, parity, and the other members of the complete set of commuting operators. The general procedure would be to continue adding basis functions to the upper and lower bases until eigenvalue differences between the upper and lower Hamiltonians accurately predict measured line positions.

The upper Hamiltonian matrix for the (5,4) band

Electronic spin S interactions with electronic orbital momentum L and nuclear orbital momentum R produce both diagonal and off-diagonal matrix elements in the Hund's case (a) representation of the Hamiltonian. The off-diagonal elements connect different basis states. For example, both of the mentioned spin orbit interactions connect $^3\Sigma^+$ and $^2\Pi$. Because van Vleck transformed Hamiltonians are not used, the appropriate parameters for the strength of these interactions are $\langle AL+ \rangle$ and $\langle BL+ \rangle$.

The presented work relies on Hamiltonians that are not parity-partitioned. Table 2 lists the molecular parameters. The values for the A 2Π state were determined utilizing the Nelder-Mead minimization algorithm using values given by Brooke, et al. [2] as trial values. Error estimates were not computed, and the values of Brooke, et al. [2] were only very slightly changed.

In Table 2, parameters not followed by a number in parenthesis were held fixed or an error estimate was not computed. The value in parenthesis is the standard deviation of the fitted value.

Table 2. Molecular parameters used in this work. A value in parenthesis indicates the standard deviation in the fitted value.

	$X^2\Sigma^+$	$B^2\Sigma^+$	$A^2\Pi$
	$v = 4$	$v = 5$	$v = 17$
B_v	1.820866(13)	1.845727(13)	1.404833
D_v	$6.172(36)\times 10^{-6}$	$8.003(38)\times 10^{-6}$	5.66×10^{-6}
A_v			-50.5253
γ_v	$-1.98(43)\times 10^{-4}$	$-1.921(44)\times 10^{-2}$	
γ_{D_v}	$-1.98(43)\times 10^{-4}$		
T_v	8011.7871	35990.1780 (25)	36010.5732
$\langle AL+ \rangle$		4.25(0.03)	
$\langle BL+ \rangle$		0.0205(0.001)	

Tables 3 and 4 show the Hamiltonian matrices for levels modeled as a mixture of $^2\Sigma^+$ and $^2\Pi$ basis states, without and with spin-orbit interactions, respectively.

Table 3: Hamiltonian matrix without spin-orbit coupling. The bottom row contains the energy eigenvalues.

				v	5	5	17	17	17	17
				Λ	0	0	-1	-1	1	1
				Σ	-0.5	0.5	-0.5	0.5	-0.5	0.5
v	Λ	Σ	Ω		-0.5	0.5	-1.5	-0.5	0.5	1.5
5	0	-0.5	-0.5		36351.6409	-25.6707	0	0	0	0
5	0	0.5	0.5		-25.6707	36351.6409	0	0	0	0
17	-1	-0.5	-1.5		0	0	36257.6340	-19.5866	0	0
17	-1	0.5	-0.5		0	2.8639	-19.5866	36310.9646	0	0
17	1	-0.5	0.5		0	2.3274	0	0	36310.9646	-19.5866
17	1	0.5	1.5		0	2.8566	0	0	-19.5866	36257.6340
				$E_{m,J}$	36377.3116	36325.9702	36251.2135	36317.3851	36317.3851	36251.2135

Table 4: Hamiltonian matrix including spin-orbit coupling, but otherwise using the same layout as in Table 3. A reduction by one order of magnitude in the standard deviation of the spectral line fitting can be accomplished when including the perturbations.

				v	5	5	17	17	17	17
				Λ	0	0	-1	-1	1	1
				Σ	-0.5	0.5	-0.5	0.5	-0.5	0.5
v	Λ	Σ	Ω		-0.5	0.5	-1.5	-0.5	0.5	1.5
5	0	-0.5	-0.5		36351.6409	-25.6707	2.8566	2.3274	2.8639	0
5	0	0.5	0.5		-25.6707	36351.6409	0	2.8639	2.3274	2.8566
17	-1	-0.5	-1.5		2.8566	0	36257.6340	-19.5866	0	0
17	-1	0.5	-0.5		2.3274	2.8639	-19.5866	36310.9646	0	0
17	1	-0.5	0.5		2.8639	2.3274	0	0	36310.9646	-19.5866
17	1	0.5	1.5		0	2.8566	0	0	-19.5866	36257.6340
				$E_{m,J}$	36377.3957	36327.7869	36250.9625	36317.3525	36315.8194	36251.1620

In Table 3, the Hamiltonian was computed for $\langle AL+ \rangle = \langle BL+ \rangle = 0$ in other words the off-diagonal spin-orbit coupling has been removed. Consequently, the 2×2 matrices along the main diagonal are independent, and could be individually diagonalized. Using matrices like these to model upper states of the CN violet (5,4) band, the 100 experimental spectral lines reported by Ram et al. [1] were fitted with standard deviation of 0.25 cm^{-1} . Standard Hund's case (a) matrix elements [10, 12] were used. In Table 4, off-diagonal spin-orbit coupling mixes the Hund's case (a) basis states, and the standard deviation of the spectral line fit mentioned in Table 3 is reduced by a factor of 10 to 0.025 cm^{-1} . The spin-orbit coupling constants $\langle AL+ \rangle = 4.25(0.03)$ and $\langle BL+ \rangle = 0.205(0.001)$ listed in Table 2 were used to determine the Hamiltonian in Table 4. This single 6×6 matrix describing ${}^2\Pi - {}^2\Sigma^+$ mixing can be compared with the two 3×3 parity partitioned matrices of Brown and Carrington [13].

A diatomic line position fitting algorithm

A basic tool for the diatomic spectroscopist is a computer program that accepts a table of experimentally measured vacuum wave numbers $\tilde{\nu}_{\text{exp}}$ versus J' and J , and outputs a set of molecular parameters with which one can reproduce the $\tilde{\nu}_{\text{exp}}$ with a standard deviation comparable to the estimated experimental error. In practice, an experimental line list frequently shows gaps, viz. spectral lines are missing. Following a successful fitting process, one can use the molecular parameters to predict all lines. A computed line list is especially useful when it includes the Condon and Shortley [14] line strength from which the Einstein coefficients and oscillator strength [15, 16] and the HITRAN line strength [17] can be calculated. A feature of the line fitting program described below is its use of non-zero rotational strengths (see Eq. (9) below) to mark which of the many computed differences between upper and lower term values represents the vacuum wavenumber of an allowed spectral line. Consequently, the fitting process creates a complete line list including rotational factors. Parity plays no part in the fitting process, but the same orthogonal matrix that diagonalizes the case (a) Hamiltonian matrix will also diagonalize the case (a) parity matrix whose elements are given in Equation (5). The $p = \pm 1$ parity eigenvalue becomes a computed quantity, and the e/f parity designation is established from the parity eigenvalue using the accepted convention Brown et al. [18].

Trial values of upper and lower state molecular parameters, typically taken from previous works [2] for the band system in question, are used to compute upper H' and lower H Hamiltonian matrices in the case (a) basis given by Eq. (4) for specific values of J' and J . The upper and lower Hamiltonians are numerically diagonalized,

$$T' = \tilde{U}' H' U' \quad (6)$$

$$T = \tilde{U} H U \quad (7)$$

giving the upper T' and T term values. The vacuum wavenumber $\tilde{\nu}$ is determined,

$$\tilde{\nu}_{ij} = T'_i - T_j, \quad (8)$$

and the rotational strength is evaluated,

$$S_{ij}(J', J) = (2J+1) \left| \sum_n \sum_m \tilde{U}'_{in} \langle J\Omega; q, \Omega' - \Omega | J'\Omega' \rangle U_{mj} \delta(\Sigma'_n \Sigma_m) \right|^2 \quad (9)$$

The degree of the tensor operator, q , responsible for the transitions amounts to $q = 1$ for electric dipole transitions. For a non-zero rotational factors, $S(J', J)$, the vacuum wavenumber is added to a table of computed line positions to be compared with the experimental list $\tilde{\nu}_{\text{exp}}$ versus J' and J . The Clebsch-Gordan coefficient, $\langle J\Omega; q, \Omega' - \Omega | J'\Omega' \rangle$, is the same one appearing in the pure case (a) - case (a) formulae for $S(J', J)$. For a specific values of J' and J , one constructs tables for $\tilde{\nu}_{\text{exp}}$ and computed $\tilde{\nu}_{ij}$. The differences $\Delta\tilde{\nu}_{ij}$

$$\Delta\tilde{\nu}_{ij} = \tilde{\nu}_{ij} - \tilde{\nu}_{\text{exp}} \quad (10)$$

are computed where each $\tilde{\nu}_{ij}$ is the one that most closely equals one of the $\tilde{\nu}_{\text{exp}}$. Once values of $\tilde{\nu}_{ij}$ and $\tilde{\nu}_{\text{exp}}$ are matched, each is marked unavailable until a new list of $\tilde{\nu}_{ij}$ is computed. The indicated computations are performed for all values of J' and J in the experimental line list, and corrections to the trial values of the molecular parameters are subsequently determined from the resulting $\Delta\tilde{\nu}_{ij}$. The entire process is iterated until the parameter corrections become negligibly small. As this fitting process successfully concludes, one obtains a set of molecular parameters that predict measured line positions, $\tilde{\nu}_{\text{exp}}$, with a standard deviations that equal the experimental estimates within the accuracy of the $\tilde{\nu}_{\text{exp}}$.

Discussion

The influence on intensities in the (5,4) band of the CN violet system caused by the weak spin-orbit mixing, Figures 1 and 2 is significantly larger than initially anticipated. This can be noticed because computation of the rotational strengths is an integral part of our line position fitting program. The eigenvectors that diagonalize the Hamiltonian to yield fitted line position $\tilde{\nu}$ also yield $S(J', J)$. In established diatomic molecular practice, Hönl-London factors are determined independently of line positions. Analytical approximations utilize the parameter $Y = A/B$ to account for the influence of spin-orbit interaction on $S(J', J)$. Kovács [19] gives many examples, Li, et al. [20] give a more recent application. These analytical approximations can accurately account for intermediate spin-orbit coupling which smooth transitions between case (a) and case (b) with increasing J' and J , but show limited sensitivity to abrupt changes in $S(J', J)$ near perturbations such as those seen the CN (5,4) band.

Conclusions

The Wigner-Witmer diatomic eigenfunction makes it possible to form an exact, mathematical connection between computation of $\tilde{\nu}$ and $S(J', J)$ in a single algorithm. The concept of the non-vanishing rotational strengths as the omnipotent selection rule initially conceived as a simplifying convenience in a computer algorithm is now seen to be more

valuable, as evidenced in this work's analysis of the CN (5,4) band perturbations by isolating a specific branch. Future work is planned for comparisons of the CN (10,10) band spectra that include perturbation and that show promising agreements with experiments and PGOPHER predictions.

Acknowledgments

One of us (CGP) acknowledges support in part by the Center for Laser and greatly thanks for the outstanding dedication of late James O. Hornkohl.

References

- Ram RS, Davis SP, Wallace L, Englman R, Appadoo DRT, Bernath PF. Fourier transform emission spectroscopy of the $B^2\Sigma^+ - X^2\Sigma^+$ system of CN. *J Mol Spectrosc*. 2006;237(2):225–231.
- Brooke JSA, Ram RS, Western CM, Li G, Schwenke DW, Bernath PF. Einstein A Coefficients and Oscillator Strengths for the $A^2\Pi - X^2\Sigma^+$ (Red) and $B^2\Sigma^+ - X^2\Sigma^+$ (Violet) Systems and Rovibrational Transitions in the $X^2\Sigma^+$ State of CN ApJS. 2014;210(2):1-15. doi:10.1088/0067-0049/210/2/23
- Western CM. PGOPHER: A program for simulating rotational, vibrational and electronic spectra. *J Quant Spectrosc Rad Transfer*. 2017;186(S1):221–242.
- Ito H, Fukuda Y, Ozaki Y, Kondow T, Kuchitsu K. Analysis of perturbation between the $v = 5$ and $v = 17$ levels of the CN radical. *J Molec Spectrosc*. 1987;121(1):84–90.
- Engleman R. The $v = 0$ and $+1$ sequence bands of the CN violet system observed during the flash photolysis of BrCN. *J Mol Spectrosc*. 1974;49(1):106–116.
- National Solar Observatory (NSO) at Kitt Peak, McMath-Pierce Fourier Transform Spectrometer (FTS) data. [cited 2016 Dec 20]; Available from: ftp://vso.nso.edu/FTS_cdrom/FTS30/920212R0.005
- Parigger CG, Woods AC, Surmick DM, Gautam G, Witte MJ, Hornkohl JO. Computation of diatomic molecular spectra for selected transitions of aluminum monoxide, cyanide, diatomic carbon, and titanium monoxide. *Spectrochim Acta Part B: At Spectrosc*. 2015;107:132–138.
- Yurchenko SN, Lodi L, Tennyson J, Stolyarov AV. Duo: a general program for calculating spectra of diatomic molecules. *Comput Phys Commun*. 2016;202:262–275.
- Wigner E, Witmer EE. On the structure of the diatomic molecular spectra according to quantum mechanics. *Z Phys*. 1928;51(11):859–886. Hetteima H. On the structure of the spectra of two-atomic molecules according to quantum mechanics. *Quantum Chemistry: Classic Scientific Papers*. World Scientific: Singapore; 2000;287–311.
- Zare RN, Schmeltekopf AL, Harrop DL, Albritton DL. A Direct Approach for the Reduction of Diatomic Spectra to Molecular Constants for the Construction of RKR Potentials. *J Mol Spectrosc*. 1973;46(1):37–66.
- Brown JM, Howard BJ. Approach to the anomalous commutator relations of rotational angular momentum in molecules. *Mol Phys*. 1976;31(5):1517–1525.
- Lefebvre-Brion H, Field RW. *The Spectra and Dynamics of Diatomic Molecules*. Elsevier: Amsterdam, 2004.
- Brown JM, Carrington A. *Rotational Spectroscopy of Diatomic Molecules*. Cambridge Univ Press: Cambridge; 2003;516–517.
- Condon EU, Shortley GH. *The Theory of Atomic Spectra*. Cambridge Univ Press: Cambridge; 1964.
- Hilborn RC. Einstein coefficients, cross sections, f values, dipole moments, and all that. *Am J Phys*. 1982;50(11):982–986.
- Thorne AP. *Spectrophysics*, 2nd ed. Chapman and Hall. New York. 1988.
- Rothman LS, Rinsland CP, Goldman A, Massie ST, Edwards DP, Flaud JM, et al. The HITRAN molecular spectroscopic database and HAWKS (HITRAN Atmospheric Workstation): 1996 Edition. *J Quant Spectrosc Rad Transfer*. 1998;60(5):665–710.
- Brown JM, Hougen JT, Huber KP, Johns JWC, Kopp I, Lefebvre-Brion H, et al. The labeling of parity doublet levels in linear molecules. *J Mol Spectrosc*. 1975;55(1-3):500–503.
- Kovács I. *Rotational Structure in the Spectra of Diatomic Molecules*. Elsevier: New York. 1969.
- Li G, Harrison JJ, Ram RS, Western CM, Bernath PF. Einstein A coefficients and absolute line intensities for the $E^2\Pi - X^2\Sigma^+$ transition of CaH. *J Quant Spectrosc Rad Transfer*. 2012;113(1):67–74.